FULL PAPER

Protein-Release Behavior of Self-Assembled PEG–β-Cyclodextrin/PEG–Cholesterol Hydrogels

By *Frank van de Manakker, Kevin Braeckmans, Najim el Morabit, Stefaan C. De Smedt, Cornelus F. van Nostrum,* and *Wim E. Hennink**

This paper reports on the degradation and protein release behavior of a self-assembled hydrogel system composed of β-cyclodextrin- (βCD) and cholesterol-derivatized 8-arm star-shaped poly(ethylene glycol) (PEG_8). By mixing βCD- and cholesterol-derivatized PEG_8 (molecular weights 10, 20 and 40 kDa) in aqueous solution, hydrogels with different rheological properties are formed. It is shown that hydrogel degradation is mainly the result of surface erosion, which depends on the network swelling stresses and initial crosslink density of the gels. This degradation mechanism, which is hardly observed for other water-absorbing polymer networks, leads to a quantitative and nearly zero-order release of entrapped proteins. This system therefore offers great potential for protein delivery.

1. Introduction

Hydrogels are three-dimensional hydrophilic networks that can absorb considerable amounts of water and are under investigation for a wide variety of pharmaceutical and biomedical applications, such as drug delivery and tissue engineering.[1–8] In particular, hydrogels provide excellent opportunities for use as protein releasing matrices, because of their high water content, good compatibility with proteins, and tailorable release kinetics. Crosslinks, which can have a chemical (covalent) or physical (reversible) nature have to be introduced between hydrophilic polymer chains to create a hydrogel structure.[5] Since chemical crosslinking presents several drawbacks, that is, the need for mostly toxic crosslinking agents or irreversible modification and aggregation of the entrapped proteins,[9–11] network preparation strategies that are based on non-permanent, reversible interactions have gained a lot of interest. Based on their self-assembling nature, physically crosslinked hydrogels have presently received attention as injectable, in situ gelling devices.[12–15] A great variety of physically crosslinked hydrogels have been reported, which are based on ionic interactions,[16,17] hydrophobic interactions,[18–20] hydrogen bonds,[21,22] crystallinity,[23] stereocomplex formation,[24–27] or specific biomimetic interactions.[28–30]

We and others recently reported on self-assembling hydrogel systems,[31–37] in which physical crosslinking is established by inclusion complex formation between β-cyclodextrin (βCD) and a complementary low molecular weight guest molecule. The cyclic oligosaccharide βCD is composed of 7 glucopyranose units that are joined by α-1,4-glucosidic linkages.[38] Driven by hydrophobic and van der Waals interactions, the relatively hydrophobic pocket of βCD serves as a reversible binding site for a wide range of lipophilic molecules (e.g., adamantane and cholesterol).[39–41]

Reversible hydrogel systems, for example, those composed of adamantane- and βCD-grafted chitosan[42] or hyaluronic acid[33,43] have been described in the literature. Also, stimuli-responsive gels were formed after combining poly(acrylamide) derivatized with either βCD or aromatic guest molecules.[34] In addition, Kretschmann et al. reported the formation of thermo-responsive gels by combining adamantane-derivatized *N*-isopropylacrylamide copolymers and a low molecular weight dimer of βCD in aqueous solution.[35]

For clinical applications, it is important that the hydrogels are biodegradable and that the formed degradation products are either metabolized or that they can be excreted by renal filtration. Many hydrogel systems have been developed that can be degraded either hydrolytically[19,44–47] or enzymatically.[48–51] For chemically degrading hydrogels, their high water content leads to degradation of the polymer chains throughout the whole matrix. Moreover, the formed degradation products can easily diffuse out of the matrix leading to hydrogel bulk erosion and release of encapsulated proteins that is often difficult to predict. Only when the water transport into the polymer network is slower than the rate of polymer chain scission, surface erosion occurs, where the loss of material is only confined to the surface of the polymer device. Although surface erosion has frequently been observed for materials made of hydrophobic polymers, such as polyanhydrides,[52] poly(adipic anhydride),[53] and poly(ortho esters),[54] it has rarely been observed for hydrogels. As one of the scarce examples, surface-eroding hydrogels based on

[*] Prof. W. E. Hennink, F. van de Manakker, N. el Morabit, Dr. C. F. van Nostrum
Department of Pharmaceutics
Utrecht Institute for Pharmaceutical Sciences (UIPS)
Utrecht University
Sorbonnelaan 16, P.O. Box 80082, 3508 TB Utrecht (The Netherlands)
E-mail: w.e.hennink@uu.nl
Prof. K. Braeckmans, Prof. S. C. De Smedt
Laboratory of General Biochemistry and Physical Pharmacy
Department of Pharmaceutics, Ghent University
Harelbekestraat 72, 9000 Ghent (Belgium)

DOI: 10.1002/adfm.200900603

fluoroalkyl-modified PEG[55] or stereocomplexed multi-block Pluronic copolymers[24] were reported, where linear mass erosion processes were attributed to a combination of polymer chain disentanglement and disruption of the closely packed micellar gel structure at the gel surface layer. For the stereocomplexed multi-block Pluronic hydrogels, the release of human growth hormone (hGH) was partially controlled by surface erosion, and followed nearly zero-order kinetics.[24] Surface erosion was also observed for physically crosslinked protein hydrogels containing leucine zipper domains.[56,57] In particular, enzymatically degradable hydrogels, for example, those composed of poly(ethylene glycol)-polycaprolactone (PCL-*b*-PEG-*b*-PCL) block copolymers[49] or peptide-cross-linked dextran,[48] degrade in a surface-eroding fashion, caused by the slow transport of the enzyme into the gel compared to the rate of enzymatic cleavage.

Recently, we reported on a self-assembling hydrogel system based on βCD/cholesterol inclusion complexes.[31,32] In this system, 8-arm star shaped poly(ethylene glycol) (PEG_8) was modified with either βCD or cholesterol functionalities via a hydrolytically cleavable succinyl linker. After dissolution of both polymeric components in an aqueous environment, a physical gel network was formed due to the formation of βCD/cholesterol inclusion complexes. The mechanical properties of this gel system are easily tailorable by a wide variety of parameters, such as temperature, polymer concentration, βCD/cholesterol stoichiometry, or the use of different PEG molecular weights and architectures.[31,32] This makes it a promising candidate for drug delivery or as scaffolding material for tissue engineering applications.

The aim of this study was to evaluate the in vitro degradation mechanism and protein release behavior of these self-assembling PEG–βCD/PEG–chol hydrogels. A series of hydrogels was prepared, which contained different concentrations of βCD- and cholesterol-derivatized 8-arm star shaped PEG with varying molecular weights (10, 20, and 40 kDa). Then, the gel mechanical properties and their dissolution kinetics were studied. Moreover, to get more insight into the protein release mechanisms, the mobility of two proteins (lysozyme and BSA) in the physical networks was investigated with fluorescence recovery measurements after photobleaching (FRAP) and experimental protein release data were fitted to well established mathematical release models.

2. Results and Discussion

2.1. Gel Mechanical Properties

For this study, star shaped 8-arm PEG with three different molecular weights (10, 20, and 40 kDa) was derivatized with either βCD or cholesterol moieties as described previously.[31] The resulting polymers will throughout be referred to as PEG_8xxK–chol or PEG_8xxK–βCD, where xx represents the PEG M_W (10, 20, or 40 kDa). These βCD- and cholesterol-functionalized PEG_8 polymers were mixed in aqueous solution to yield physically crosslinked polymer networks. All mixtures could be considered as 'hydrogels' at room temperature, according to a commonly used vial tilting method.[58,59] Equimolar amounts of βCD- and cholesterol-groups were used in the mixtures, because we have previously shown that gels obtained with this ratio gave the highest G' (storage modulus) values.[31]

Table 1 gives the composition of the 22.5% and 35% (w/w) PEG_8–βCD/PEG_8–chol hydrogel systems investigated in this study. Table 1 shows the rheological properties of the different hydrogels at 37 °C. At this temperature, the highest storage moduli (G') were observed for the $PEG_8$10K–βCD/$PEG_8$20K–chol mixtures followed by the $PEG_8$20K–βCD/$PEG_8$20K–chol mixtures. Moreover, the storage moduli (G') of these gels exceeded the loss moduli (G''), which indicates that these gels have typical viscoelastic properties. For the $PEG_8$10K- and $PEG_8$40K-based systems, G' did not exceed G'', which indicates that at 37 °C they mainly have viscous characteristics. The low gel strength of these $PEG_8$10K and $PEG_8$40K systems compared to the gels consisting of derivatized $PEG_8$20K has been explained by their lower crosslink density.[31] A network composed of derivatized $PEG_8$40K comprises lower concentrations of βCD and cholesterol groups than networks of lower molecular weight PEG_8 and will therefore result in weaker hydrogels. In the case of $PEG_8$10K-based mixtures, the lower aqueous solubility of the $PEG_8$10K–chol component decreases the number of cholesterol units available for inclusion complex formation, which leads to imperfect networks. This also explains why the strongest gels are obtained after combining $PEG_8$10K–βCD and $PEG_8$20K–chol in aqueous solution. Here, the use of a larger PEG_8–chol component (20 kDa instead of 10 kDa) reduces potential insolubility issues as observed with the

Table 1. Composition and rheological characteristics (mean ± standard deviation, $n = 3$) of the 8-arm βCD- and cholesterol-derivatized PEG based hydrogels.

Gel composition	DS PEG_8–βCD [a]	DS PEG_8–chol [a]	Polymer content [% (w/w)]	G' [kPa] [b]	G'' [kPa] [b]	T_{gel} [°C]
$PEG_8$10K–βCD/$PEG_8$10K–chol	7.8 ± 0.1	5.6 ± 0.1	22.5	0.08 ± 0.01	0.06 ± 0.02	17 ± 1
			35	0.21 ± 0.08	0.3 ± 0.1	33 ± 1
$PEG_8$20K–βCD/$PEG_8$20K–chol	7.7 ± 0.3	5.6 ± 0.4	22.5	4.5 ± 0.8	3.5 ± 0.3	38 ± 1
			35	12.9 ± 0.7	11.6 ± 1.3	48 ± 2
$PEG_8$40K–βCD/$PEG_8$40K–chol	7.7 ± 0.3	5.9 ± 0.3	22.5	0.51 ± 0.05	0.54 ± 0.04	30 ± 2
			35	0.7 ± 0.3	1.4 ± 0.5	24 ± 1
$PEG_8$10K–βCD/$PEG_8$20K–chol	7.8 ± 0.1	5.7 ± 0.5	22.5	8.4 ± 0.8	8.0 ± 0.6	39 ± 1
			35	38 ± 3	27 ± 3	43 ± 1

[a] Degree of substitution (DS) defined as the number of either cholesterol or βCD molecules per PEG_8 molecule determined by ^{1}H NMR spectroscopy or polarimetry.[31] [b] Determined at 37 °C.

$PEG_8$10K–chol component,[31] while the use of the low molecular weight $PEG_8$10K–βCD component increases the concentration of interacting groups, leading to tighter networks.

It has been previously demonstrated that PEG_8–βCD/PEG_8–chol gels are thermoreversible, due to their physical nature.[31,32] While heating a viscoelastic gel mixture with $G' > G''$, a gel-to-sol transition occurs at its gel transition temperature (T_{gel}), where G' equals G''. Above T_{gel}, G'' starts to dominate, which means that the mixtures behave as viscous liquids. Table 1 lists T_{gel} for all mixtures. It shows that the $PEG_8$10K–βCD/$PEG_8$20K–chol and $PEG_8$20K–βCD/$PEG_8$20K–chol systems have T_{gel} exceeding body temperature, meaning that the mixtures keep their viscoelastic properties at 37 °C. For the gels based on $PEG_8$40K and $PEG_8$10K, the determined T_{gel} values were lower than 37 °C, which explains their mainly viscous behavior at this temperature. The G'' of these gel mixtures was however considerably higher compared to solutions of non-functionalized $PEG_8$10K–OH or $PEG_8$40K–OH, indicating that also in these systems interactions between the cholesterol- and βCD-moieties occur. For example, at 37 °C, G'' values for 22.5% and 35% (w/w) non-functionalized $PEG_8$10K–OH and $PEG_8$40K–OH solutions were in the range of 0.1–1 Pa, while mixtures of cholesterol- and βCD-derivatized $PEG_8$10K and $PEG_8$40K polymers resulted in G'' values from 60 to 1 400 Pa. Table 1 also demonstrates that with increasing the polymer concentration from 22.5% to 35% (w/w), G', G'', and T_{gel} significantly increases. This indicates that increasing polymer concentrations lead to stronger hydrogels. Higher concentrations of the dissolved polymer create a higher effective cross-link density and therefore tighter networks.[31,32]

2.2. Hydrogel Dissolution

The stability of the PEG_8–βCD/PEG_8–chol hydrogel system in physiological buffer was investigated. Cylindrical gels (300 mg; diameter 6.5 mm) were prepared in glass HPLC vials, and their weight change was followed after the addition of PBS containing 0.02% (w/w) sodium azide (PBS/NaN_3) on top of the gels and subsequent refreshments of this buffer over time. In this experimental setup, only the upper surface of the hydrogel cylinder is directly exposed to the buffer. Figure 1 shows the weight decrease of $PEG_8$20K–βCD/$PEG_8$20K–chol hydrogels varying in polymer concentration as a function of time. It demonstrates that after an initial swelling of the gels, they start to dissolve. It is also clear that gels with higher polymer concentrations are more stable (here, up to 6 days) and show a higher initial swelling than systems made at lower polymer concentrations. The stability of the hydrogels was also studied in serum and tissue culture medium. It was found that neither the initial swelling nor the dissolution rate of the gels is significantly different than the degradation characteristics of the gels observed in plain buffer. Figure 2 shows the dry weight of both a quickly and slowly dissolving $PEG_8$20K–βCD/$PEG_8$20K–chol hydrogel during incubation in buffer. This figure shows that the dry weight of the gels linearly decreases with time, pointing to a surface erosion process.

To evaluate this hydrogel degradation behavior in more detail, the large dye molecule, Dextran Blue, was entrapped in the gels and degradation experiments were similarly performed as described above. Dextran Blue has a large molecular weight of 2 MDa, and consequently this molecule is most likely immobile inside the network and can therefore only be released after dissolution of the gel. Figure 3 shows the time-dependent volume change of a 22.5% (w/w) $PEG_8$10K–βCD/$PEG_8$20K–chol gel loaded with 1% (w/w) Dextran Blue once exposed to buffer. It visualizes that, in agreement with the swelling data presented in Figure 1, the gel first slightly swells, after which it starts to dissolve and fully degrades in typically 10 days. Apparently, the time-dependent decrease in hydrogel volume is the result of polymer dissolution at the upper surface of the gel. As chemical cleavage (ester hydrolysis) of the interacting groups would rather lead to bulk erosion than to the surface erosion found for the PEG_8–βCD/PEG_8–chol gels (Fig. 3), this suggests that chemical degradation of the system is minimal within the experimental time scale.

Figure 4A and B display the weight decrease of Dextran-Blue-loaded gels composed of derivatized PEG_8 (22.5% and 35% (w/w)) with different molecular weights (see Table 1) after exposure to buffer. For 22.5% (w/w) hydrogels based on 8-arm PEG with molecular weights of 10 kDa, 20 kDa, 10 kDa/20kDa (1:2 (w/w) mixture), and 40 kDa, gel dissolution times of 2, 5, 8, and 14 days were found, respectively. For the 35% (w/w) hydrogels, the dissolution times increased to 4, 8, 15, and 22 days. For all gels, an increase of the polymer concentration from 22.5% to 35% (w/w)

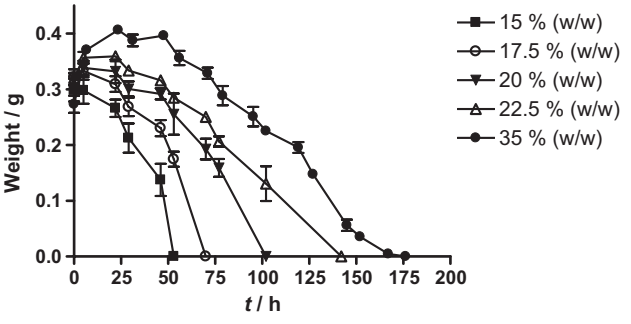

Figure 1. Weight change over time of $PEG_8$20K–βCD/$PEG_8$20K–chol hydrogels at physiological conditions (PBS, pH 7.4, 37 °C) as a function of the polymer concentration ($n = 3$).

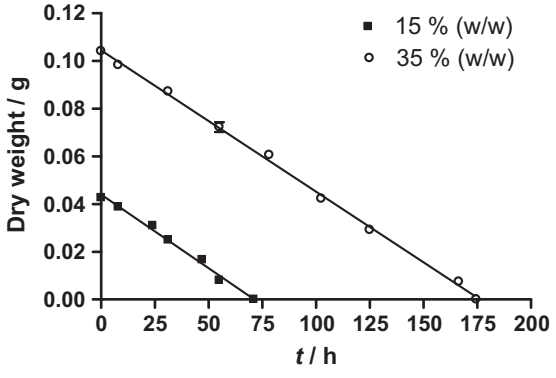

Figure 2. Time-dependent dry weight of 15% (w/w) and 35% (w/w) $PEG_8$20K–βCD/$PEG_8$20K–chol hydrogels ($n = 3$) after incubation in 5 mM NH_4OAc buffer (pH 4.7) at 37 °C.

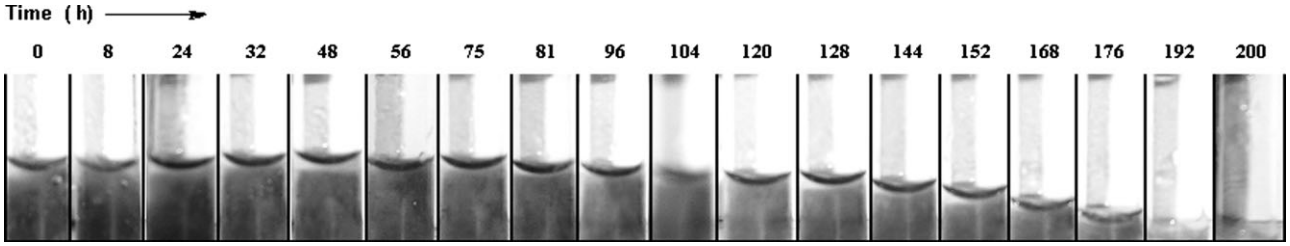

Figure 3. Volume change in time (h) at physiological conditions (PBS, pH 7.4, 37 °C) of a 22.5% (w/w) $PEG_8$10K–βCD/$PEG_8$20K–chol hydrogel loaded with 1% (w/w) Dextran Blue.

leads to a higher degree of swelling and a 1.3- to 2-fold prolongation of their dissolution time. Moreover, it is shown that changing the molecular weight of the used PEG_8's significantly influences the gel swelling and erosion profile.

In line with their relatively weak gel mechanical properties (see Section 2.1) at 37 °C, the least stable gels are those based on derivatized $PEG_8$10K (stable for 2–4 days). Hardly any swelling phase was observed for these gels, which can likely be ascribed to the rate of network dissolution being faster than the rate of water uptake. Compared to these $PEG_8$10K-based mixtures, gels composed of derivatized $PEG_8$20K or a combination of $PEG_8$10K–βCD and $PEG_8$20K–chol were more stable. The mechanically strongest $PEG_8$10K–βCD/$PEG_8$20K–chol gels (dissolution time: 8–15 days) degraded slower than those solely consisting of derivatized $PEG_8$20K (dissolution time: 5–8 days), which indicates that the initial hydrogel network density is an important factor that determines the rate of hydrogel dissolution. Although the $PEG_8$40K-based mixtures did not result in strong gels at 37 °C (see Section 2.1), they demonstrated the highest stability (dissolution times of 14 and 22 days for the 22.5% and 35% (w/w) gels, respectively). These unexpectedly slow dissolution kinetics can likely be explained by the relatively low network swelling stresses that arise in the systems after incubation with buffer as compared to hydrogels composed of 8-arm PEG with shorter chains. After absorption of water, swelling stresses are accumulating, which act as an opposing force against the inclusion complexes that hold the gel together. When these swelling stresses are high, the polymer chains release this stress mainly by dissociation of βCD/cholesterol complexes, eventually leading to fast dissolution of the gels. Because the arms of the $PEG_8$40K polymers are larger and therefore more flexible than those of the $PEG_8$10K and $PEG_8$20K polymers, they are able to relieve part of the swelling stresses without the need for breaking the βCD/cholesterol complexes. Consequently, the $PEG_8$40K-based mixtures end up with a higher number of βCD/cholesterol interactions in the swollen network, which will slow down the hydrogel erosion.

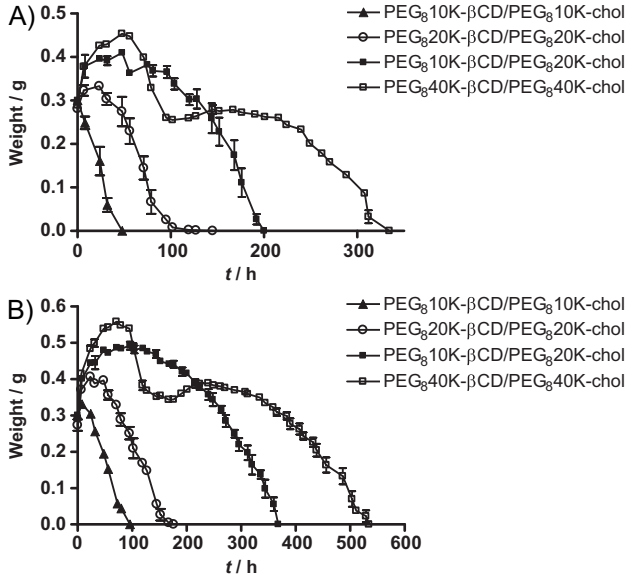

Figure 4. Time-dependent weight change of A) 22.5% (w/w) and B) 35% (w/w) Dextran Blue loaded hydrogels containing derivatized 8-arm PEG's with different molecular weights at physiological conditions (PBS, pH 7.4, 37 °C) ($n = 3$).

Figure 4A and B also shows that besides hydrogel swelling directly after adding buffer, the 22.5% and 35% (w/w) $PEG_8$40K-based mixtures start to swell again after 100 and 200 h, respectively. This demonstrates again that dissolution of derivatized $PEG_8$40K polymers only occurs at relatively high swelling stresses, where the relaxation of PEG-arms cannot be established without dissociation of βCD/cholesterol inclusion complexes. After network swelling and dissolution of the polymers at the gel's top layer, the remaining network in the bulk of the gel adopts a new swollen state, where swelling stresses accumulate till these are high enough to cause dissociation of the βCD/cholesterol interactions and concomitant hydrogel dissolution.

Besides the swelling/dissolution analysis of these different hydrogels, the Dextran Blue released in the added PBS/NaN_3 medium was also followed in time. Figure 5 shows the cumulative release of Dextran Blue from the 22.5% and 35% (w/w) hydrogels composed of 8-arm PEG with different molecular weights. It demonstrates that Dextran Blue is constantly released from the investigated gels over time and eventually 100% release of the loaded amount is reached. Furthermore, it is clear that the use of different star PEG molecular weights or increasing the polymer concentration influences the release kinetics of Dextran Blue. For every gel composition, the release kinetics of Dextran Blue correlated well with their time-dependent weight decrease, which is shown in Figure 4. This demonstrates again that the gel degradation is mainly mediated by polymer surface erosion and that the assumption of Dextran Blue being immobile in the hydrogel network is correct. This was further investigated by fitting

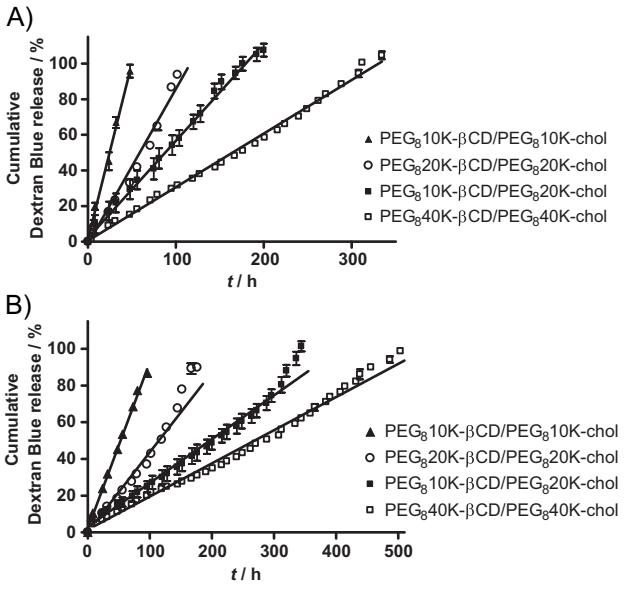

Figure 5. Release of Dextran Blue from A) 22.5% (w/w) and B) 35% (w/w) hydrogels composed of derivatized 8-arm PEG's with different molecular weights ($n = 3$).

the experimental Dextran Blue release data to the Ritger–Peppas equation:[60,61]

$$\frac{M_t}{M_\infty} = kt^n \quad (1)$$

where M_t/M_∞ represents the fractional release of the entrapped compound, k is a kinetic constant, t is the release time and n is the diffusional exponent that can be related to the release mechanism of the entrapped molecules. When $n = 0.5$, the release is completely controlled by Fickian diffusion. When $n = 1$, however, the release is governed by the swelling-induced polymer chain relaxation and subsequent gel surface erosion, which leads to zero-order release. Values of n between 0.5 and 1 indicate that both transport mechanisms play a role. For the Dextran Blue release profiles of Figure 5, n values between 0.95 and 1.00 were obtained, which confirms again that Dextran Blue is immobilized inside the hydrogel and is released at zero-order kinetics due to surface erosion of the hydrogel material.

2.3. Protein Mobility in PEG_8–βCD/PEG_8–Chol Networks

To study the mobility of two model proteins, i.e. lysozyme (M_W: 14.7 kDa, hydrodynamic diameter 4.1 nm[62]) and BSA (M_W: 67 kDa, hydrodynamic diameter 7.2 nm[62]) in the 22.5% and 35% (w/w) PEG_8–βCD/PEG_8–chol hydrogels, fluorescence recovery measurements after photobleaching (FRAP) were performed at 37 °C. Diffusion coefficients were calculated by fitting the experimental recovery curves with a previously described FRAP model.[63] Also, diffusion coefficients of these proteins were determined in solutions of the non-functionalized 8-arm PEG's and in buffer only.

Figure 6A shows a representative fluorescence recovery of FITC-labeled BSA in both a solution of non-functionalized $PEG_8$10K–OH and in a $PEG_8$10K–βCD/$PEG_8$10K–chol gel matrix. After photobleaching of FITC–BSA in a solution of non-functionalized 8-arm PEG, the fluorescence completely recovered and a diffusion coefficient of $2.6 \pm 0.3\ \mu m^2\ s^{-1}$ was calculated. However, no fluorescence recovery was observed in the FITC–BSA-loaded hydrogel matrix within the experimental time scale (15 minutes), indicating that BSA is immobile inside the hydrogel network, which suggests that the average size of the polymer network pores is smaller than the hydrodynamic diameter of BSA (7.2 nm[62]). Similar to this typical example, the immobility of FITC–BSA was also observed in the other hydrogel compositions described in Table 1.

Figure 6B shows the fluorescence recovery curves of FITC–lysozyme in an aqueous solution of non-functionalized $PEG_8$10K–OH and $PEG_8$20K–OH (1:2 (w/w)) and in a $PEG_8$10K–βCD/$PEG_8$20K–chol hydrogel. From a best fit of the FRAP model, a mobile fraction of 1.0 ± 0.1 was found for both curves. However, the diffusion coefficient in the PEG_8–OH solution was 5 times higher compared to the hydrogel. This indicates that although

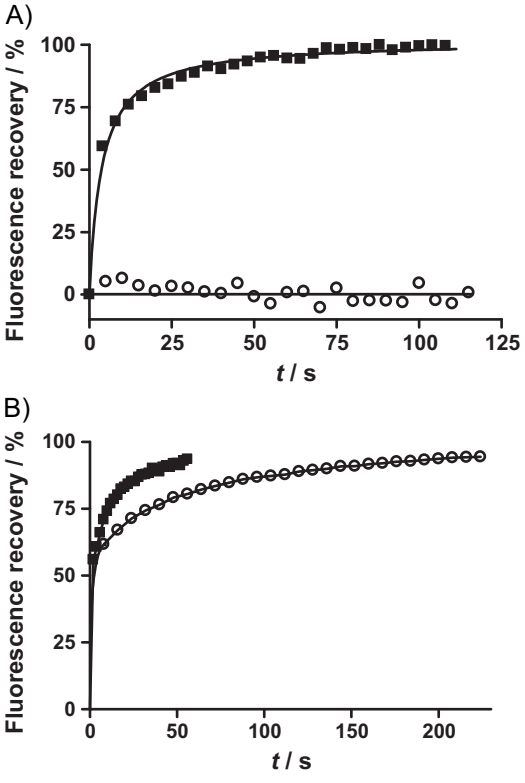

Figure 6. Typical fluorescence recovery curves after photobleaching of A) FITC–BSA in a 35% (w/w) $PEG_8$10K–OH solution (■) and a 35% $PEG_8$10K–βCD/$PEG_8$10K–chol mixture (○), and of B) FITC–lysozyme in a 35% (w/w) $PEG_8$10K–OH/$PEG_8$20K–OH (1:2 (w/w)) solution (■) and a 35% (w/w) $PEG_8$10K–βCD/$PEG_8$20K–chol mixture (○). Curves are normalized to the fluorescence immediately after bleaching. Solid lines are a best fit of the experimental data to the FRAP model.

FITC–lysozyme is not completely immobilized, the polymer network formation significantly slows down its mobility.

Previously, diffusion coefficients at room temperature of BSA and lysozyme in water were reported as 59 μm^2 s^{-1}[64] and 104 μm^2 s^{-1},[65] respectively. By extrapolating these diffusion coefficients (D) to 37 °C by using the Stokes–Einstein relation $D\eta/T$ = constant,[62,64,66] expected diffusion coefficients for BSA and lysozyme in aqueous solution at 37 °C are approximately 91 μm^2 s^{-1}[67] and 160 μm^2 s^{-1}, respectively. Table 2 lists the diffusion coefficients of FITC–BSA and FITC–lysozyme in solutions of non-functionalized 8-arm PEG with different molecular weights and in the corresponding hydrogel mixtures composed of PEG_8–βCD and PEG_8–chol. This table shows that the diffusion coefficients of both proteins in solutions of non-functionalized 8-arm PEG were 10–200-fold lower than in buffer. This can be fully explained by the higher viscosity of the polymer solutions (12–210 mPa s, Supporting Information) compared to buffer (~1 mPa s).

Table 2 also shows that the lysozyme diffusion coefficient in the hydrogels was lower than in the corresponding non-functionalized PEG_8 solutions. This demonstrates that the diffusional mobility of FITC–lysozyme in the PEG_8–βCD/PEG_8–chol gels is affected by both the high viscosity of the derivatized PEG and the establishment of a polymer network. The lowest diffusional mobility of lysozyme was observed in the $PEG_8$10K–βCD/$PEG_8$20K–chol gel mixtures, in line with its highest mechanical strength and thus the highest cross-link density of these gel mixtures (see Section 2.1). For the 22.5% (w/w) gels, lysozyme had approximately the same diffusion coefficients in the $PEG_8$40K–βCD/$PEG_8$40K–chol, the $PEG_8$20K–βCD/$PEG_8$20K–chol and the $PEG_8$10K–βCD/$PEG_8$10K–chol mixtures (D 7.6 ± 0.6 μm^2 s^{-1}, 10 ± 3 μm^2 s^{-1}, and 11 ± 2 μm^2 s^{-1}, respectively). Increasing the polymer concentration from 22.5% to 35% (w/w) resulted in a decrease of the protein's mobility. In the case of 35% (w/w) gels, the diffusion coefficient of lysozyme in the $PEG_8$40K–βCD/$PEG_8$40K–chol mixture (D 2.4 ± 0.2 μm^2 s^{-1}) was slightly higher than that in the $PEG_8$20K–βCD/$PEG_8$20K–chol (D 1.1 ± 0.3 μm^2 s^{-1}) and $PEG_8$10K–βCD/$PEG_8$10K–chol (D 1.5 ± 0.1 μm^2 s^{-1}) mixtures.

Because the gels composed of derivatized $PEG_8$40K and $PEG_8$10K have lower strengths than $PEG_8$20K-based gels (G' is 9–60 fold lower; Table 1) due to the lower network densities, the diffusional mobility of lysozyme in the relatively weak $PEG_8$40K- and $PEG_8$10K-based gel mixtures was expected to be higher than in the networks composed of functionalized $PEG_8$20K. However, the lysozyme mobility in the $PEG_8$40K-based gels is unexpectedly low (e.g., $D = 7.6 \pm 0.6$ μm^2 s^{-1} and 10 ± 3 μm^2 s^{-1} for a 22.5% (w/w) $PEG_8$40K- and $PEG_8$20K-based gel, respectively; Table 2), and is likely caused by the higher viscosity of the βCD- and cholesterol-derivatized $PEG_8$40K chains compared to the functionalized PEG_8 polymers of lower molecular weights. For the $PEG_8$10K–βCD/$PEG_8$10K–chol gels, the lysozyme diffusion coefficients being almost equal to those in the $PEG_8$20K-based gels (Table 2), give evidence that despite the low gel strengths due to imperfect network formation, these mixtures might still contain local domains in which the cross-link density is very high.

It has previously been demonstrated that a variety of aromatic dye molecules might also form inclusion complexes with βCD.[68,69] To rule out the possibility that the FITC-labeled proteins form complexes with the PEG_8–βCD gel component, which would lead to underestimated protein diffusion coefficients, fluorescence recovery measurements of FITC–lysozyme and FITC–BSA were also performed in 22.5% and 35% (w/w) solutions containing $PEG_8$20K–βCD together with $PEG_8$20K–OH (1:1 (w/w)). The solutions' viscosities were also determined (see Supporting Information). The diffusion coefficients of BSA and lysozyme in these mixtures were about 1.5–2.5 fold lower than in solutions of only $PEG_8$20K–OH. For example, the diffusion coefficient of FITC–lysozyme was 9 ± 1 μm^2 s^{-1} in a 22.5% (w/w) solution of $PEG_8$20K–βCD/$PEG_8$20K–OH (1:1 (w/w)) and 14 ± 1 μm^2 s^{-1} in a 22.5% (w/w) $PEG_8$20K–OH solution. This

Table 2. Diffusion coefficients (D, mean ± standard deviation) at 37 °C of FITC-labeled lysozyme and BSA in solutions of non-derivatized PEG and in the PEG_8–βCD/PEG_8–chol gels ($n = 5$).

Solutions/gels	Polymer concentration [% (w/w)]	FITC–lysozyme D [μm^2 s^{-1}]	FITC–BSA D [μm^2 s^{-1}]
$PEG_8$10K–OH	22.5	21 ± 1	9.4 ± 0.3
	35	6.6 ± 0.5	2.6 ± 0.3
$PEG_8$10K–βCD/$PEG_8$10K–chol	22.5	11 ± 2	nd [a]
	35	1.5 ± 0.1	nd [a]
$PEG_8$20K–OH	22.5	14 ± 1	4.6 ± 0.4
	35	2.0 ± 0.3	1.2 ± 0.2
$PEG_8$20K–βCD/$PEG_8$20K–chol	22.5	10 ± 3	nd [a]
	35	1.1 ± 0.3	nd [a]
$PEG_8$40K–OH	22.5	10 ± 1	2.4 ± 0.3
	35	2.3 ± 0.2	0.53 ± 0.02
$PEG_8$40K–βCD/$PEG_8$40K–chol	22.5	7.6 ± 0.6	nd [a]
	35	2.4 ± 0.2	nd [a]
$PEG_8$10K–OH/$PEG_8$20K–OH (1:2 (w/w))	22.5	13 ± 1	4 ± 1
	35	3.8 ± 0.4	1.7 ± 0.2
$PEG_8$10K–βCD/$PEG_8$20K–chol	22.5	4.5 ± 0.4	nd [a]
	35	0.62 ± 0.06	nd [a]

[a] Diffusion coefficients for FITC–BSA in the PEG_8–βCD/PEG_8–chol mixtures could not be determined (nd), because of the protein's extremely low mobility inside these mixtures (also see Fig. 6A).

decrease can be entirely attributed to the difference in viscosities, which was 21 ± 1 mPa s for the solution containing $PEG_8$20K–βCD/$PEG_8$20K–OH (1:1 (w/w)) and 14 ± 1 mPa s for the solution containing only $PEG_8$20K–OH. It can therefore be concluded that interactions between the FITC-labeled proteins and $PEG_8$20K–βCD do not occur.

2.4. Protein Release

To study the release of proteins from the different hydrogel compositions, three model proteins lysozyme, BSA and IgG with increasing molecular weights (14.7, 67, and 150 kDa) and hydrodynamic diameters (4.1, 7.2, and 10.7 nm[62]) were selected and loaded inside different hydrogels. Release experiments were performed in a previously described release device[62] with cylindrically shaped gels (volume 0.5 mL; diameter 8.5 mm), of which only the upper surface is in direct contact with the added release buffer, similarly as in the discussed stability experiments.

Figure 7 shows the release of lysozyme, BSA, and IgG from 22.5% (w/w) $PEG_8$20K–βCD/PEG20K–chol hydrogel cylinders. The gels showed a sustained release of the entrapped proteins during a period of more than nine days, after which the gels were completely dissolved in the release buffer. Although the used proteins have different hydrodynamic diameters, they were released at almost the same rate. These observations suggest that protein release is mainly due to surface erosion of the hydrogel. The higher release rate between 0 and 30 h after the addition of buffer can be explained by an artifact of the release device. In the release device[62] used for the protein release studies, the initial swelling of the gels as shown in the previous swelling/dissolution studies caused the hydrogel to ''swell out'' of the gel compartment, which led to a temporary larger hydrogel surface exposure to buffer and consequently faster surface erosion kinetics and protein release. After 30 h, the height of the gels was lower than that of the gel compartment in the device, so that their buffer-exposed upper surface and thus the surface erosion kinetics stayed constant during the remaining release study resulting in the observed constant protein release.

Importantly, the PEG_8–βCD/PEG_8–chol gels showed quantitative protein release, which suggests that in this system irreversible protein aggregation and precipitation does not occur. Further, no significant differences in specific enzymatic activity were found between released lysozyme and freshly dissolved protein, which demonstrates that the structural integrity of the protein was preserved, emphasizing the protein-friendly character of the PEG_8–βCD/PEG_8–chol hydrogel system.

FRAP data showed that BSA was immobile inside the hydrogels, which shows that BSA and also the larger protein IgG can only be released upon gel surface erosion, leading to the nearly zero-order release profiles of these proteins. However, the FRAP experiments showed that lysozyme still has some mobility inside the various network compositions, so that the observed nearly zero-order release profiles of this protein were not immediately expected. To get more insight into the contributions of both Fickian diffusion and the polymer surface erosion on the observed lysozyme release, experimental release data were compared to lysozyme release curves that were predicted by the early-time approximation equation of Fick's second law:[60]

$$\frac{M_t}{M_\infty} = 4\sqrt{\frac{Dt}{\pi\delta^2}} \quad (2)$$

where M_t/M_∞ represents the fractional release of the entrapped protein, D is the diffusion coefficient determined using FRAP experiments, t is the release time, and δ is the diffusional distance, which is twice the height of the hydrogel cylinder (2×8.8 mm), because protein diffusion is restricted only to the upper surface of the gel.

Figure 8 shows the cumulative release of lysozyme from 22.5% and 35% (w/w) $PEG_8$10K–βCD/$PEG_8$20K–chol gels. This figure shows that an increase of the polymer solid content from 22.5% to 35% (w/w) prolonged the lysozyme release from about 6 to 11 days. This can be related to the slower surface erosion, as described in Section 2.2. Besides the experimentally observed release profiles, Figure 8 also shows the lysozyme release curves for both gels as predicted by Equation 2. It is clear that lysozyme release from the surface-eroding $PEG_8$10K–βCD/$PEG_8$20K–chol hydrogels was four- to eight-fold faster than would be the case for Fickian diffusion only. This was also true for the other hydrogel compositions. The differences between the empirical release patterns and the mathematical release model based on diffusion explain that, although diffusional processes might partially contribute to the release of lysozyme, the hydrogel surface erosion is mainly governing its release.

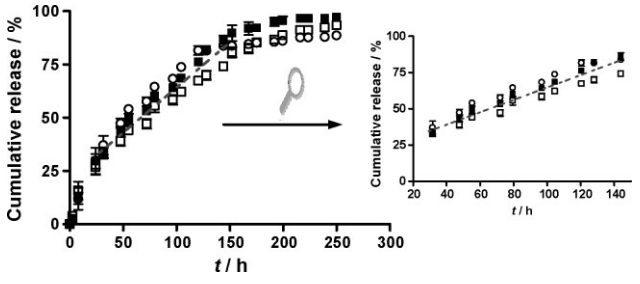

Figure 7. Release of lysozyme (■), BSA (○) and IgG (□) from 22.5% (w/w) $PEG_8$20K–βCD/$PEG_8$20K–chol hydrogels in PBS (pH 7.4) at 37 °C ($n = 3$).

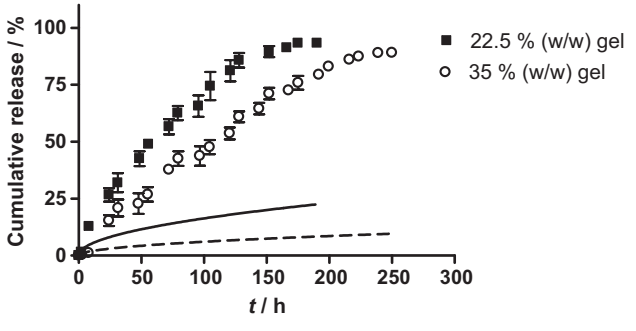

Figure 8. Release of lysozyme from 22.5% (w/w) (■) and 35% (w/w) (○) $PEG_8$10K–βCD/$PEG_8$20K–chol hydrogels in PBS (pH 7.4) at 37 °C ($n = 3$). Solid and dashed lines are the release kinetics predicted from Equation 2 for the 22.5% and 35% gels, respectively.

Table 3. Diffusional exponents *n* for the release of lysozyme from the different hydrogel compositions, determined by fitting Equation 1 to the experimentally observed lysozyme release kinetics.

Gel composition	Polymer concentration [% (w/w)]	*n*	R^2
$PEG_8$20K–βCD/$PEG_8$20K–chol	22.5	0.59 ± 0.01	0.99
	35	0.71 ± 0.02	0.99
$PEG_8$10K–βCD/$PEG_8$10K–chol	22.5	0.50 ± 0.01	1.00
	35	0.63 ± 0.02	0.98
$PEG_8$40K–βCD/$PEG_8$40K–chol	22.5	0.59 ± 0.01	0.99
	35	0.68 ± 0.02	0.99
$PEG_8$10K–βCD/$PEG_8$20K–chol	22.5	0.67 ± 0.02	0.99
	35	0.80 ± 0.02	0.99

To investigate the influence of the gel composition on the release mechanism of lysozyme, the experimental lysozyme release from the different hydrogels (data points between $t = 0$–30 h excluded) were fitted to Equation 1 [60,61] to obtain the diffusional exponents *n*. Table 3 shows that all mixtures lead to *n* values between 0.5 and 1, which means that the lysozyme release is a combination of diffusional processes and surface erosion. Moreover, an increase of the polymer concentration from 22.5% to 35% (w/w) leads to higher diffusional exponents, which demonstrates that the lysozyme release becomes more erosion dependent at higher polymer concentrations. Higher polymer concentrations lead to tighter networks, in which the diffusion of lysozyme is lower as well. For the lysozyme release from the 22.5% $PEG_8$10K–βCD/$PEG_8$10K–chol mixture, a diffusional exponent of 0.50 ± 0.01 was found. This means that for this particular hydrogel system, the lysozyme release is controlled by diffusion. With the experimental release data and Equation 2, the diffusion coefficient for lysozyme in this gel was calculated to be 130 ± 20 $\mu m^2 s^{-1}$, which is 10 times higher than the diffusion coefficient determined during the FRAP measurements (11 ± 2 $\mu m^2 s^{-1}$). This higher protein mobility is most likely the result of a swelling-induced increase of the hydrogel pore size.

In Figure 9, the release of the small peptide Bradykinin[70] (1.1 kDa) from 22.5% and 35% (w/w) $PEG_8$20K–βCD/$PEG_8$20K–chol gels is shown. When increasing polymer concentration from 22.5% to 35%, the Bradykinin release was slowed down. Both curves were fitted to Equation 1, which yielded diffusional exponents of 0.50 ± 0.01 and 0.59 ± 0.01 for respectively the 22.5% and 35% (w/w) mixtures. This shows that, by using high enough polymer concentrations, it is even possible to make the release of this small peptide partially dependent on the hydrogel surface erosion, although the release of this low molecular weight compound mainly follows first-order kinetics.

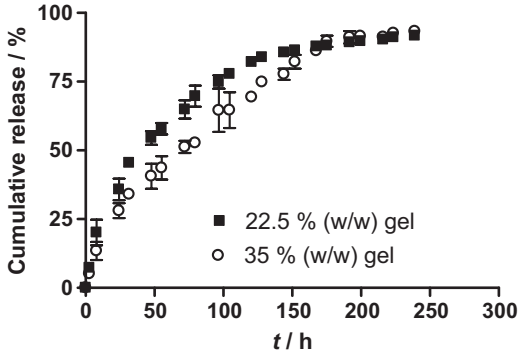

Figure 9. Release of Bradykinin from 22.5% (w/w) and 35% (w/w) $PEG_8$20K–βCD/$PEG_8$20K–chol hydrogels in PBS (pH 7.4) at 37 °C ($n = 3$).

3. Conclusions

In this study, the degradation and protein release behavior of novel self-assembling hydrogels based on βCD/cholesterol interactions was investigated. Hydrogels were composed of βCD- and cholesterol-derivatized 8-arm star shaped PEG with increasing molecular weights (10, 20, and 40 kDa). Hydrogel degradation was mediated by a surface erosion mechanism, which is controlled by a combination of network swelling stresses and the initial cross-link density of the gels. Dependent on the hydrogel composition, the hydrogel surface dissolution also substantially controlled the release of proteins from the gels, which resulted in continuous, nearly zero-order release patterns of entrapped proteins. These unique protein release characteristics as well as its tailorable mechanical properties[31] and the previously reported biocompatibility of PEG-based hydrogels,[2] makes this system very useful as a drug delivery matrix or for other pharmaceutical and biomedical applications.

4. Experimental

Materials: Star shaped 8-arm poly(ethylene glycol)s (PEG_8–OH) were purchased from JenKem Technology USA (Allen, USA). Products with various M_W were used; $PEG_8$10K–OH ($M_n = 9\,656$ Da (MALDI), PDI = 1.10), $PEG_8$20K–OH ($M_n = 20\,185$ Da (MALDI), PDI = 1.08) and $PEG_8$40K–OH ($M_n = 42\,680$ Da (MALDI), PDI = 1.06). Dextran Blue from Leuconostoc ssp. ($M_r \sim 2\,000\,000$ Da) and lysozyme from hen egg white were obtained from Fluka (Buchs, Switzerland). Bovine serum albumin (BSA), immunoglobulin G (IgG) from human serum, fluorescein isothiocyanate bovine serum albumin (FITC–BSA), Bradykinin acetate, fluorescein isothiocyanate isomer I (FITC), sodium azide (NaN_3) and trifluoroacetic acid (TFA) were provided by Sigma-Aldrich (Zwijndrecht, The Netherlands). *N*-2-hydroxyethylpiperazine-*N*'-2-ethanesulfonic acid (HEPES) and ammonium acetate (NH_4OAc) were obtained from Acros Chimica (Geel, Belgium) and Merck (Darmstadt, Germany), respectively. Phosphate buffered saline (PBS (10.5 mM phosphate; 140.3 mM NaCl), pH 7.4) was purchased from Braun Melsungen AG (Melsungen, Germany), acetonitrile (ACN) from Biosolve Ltd. (Valkenswaard, The Netherlands) and the bicinchoninic acid protein assay kit (BCA Protein Assay) from Pierce Biotechnology Inc. (Rockford, USA).

Polymer Synthesis: Star shaped 8-arm poly(ethylene glycol)s (PEG_8-OH) with molecular weights of 10, 20, and 40 kDa were derivatized with either cholesterol or β-cyclodextrin (βCD) moieties using a biodegradable succinyl linker (SA) and characterized as previously reported [31]. The degree of substitution (DS) is defined as the number of either cholesterol or βCD molecules per PEG molecule. A specific polymer is referred to as PEG_8xxK–chol or PEG_8xxK–βCD, where xx represents the PEG M_W (10, 20, or 40 kDa).

Hydrogel Preparation: PEG_8–cholesterol and PEG_8–βCD mixtures (molar ratio cholesterol/βCD = 1) were dissolved in 5 mM NH_4OAc buffer (pH 4.7) to obtain 2% (w/w) solutions. These solutions were then lyophilized and hydrogels were obtained by hydration of the lyophilized mixtures for 16 hours at 4 °C with appropriate volumes of PBS containing 0.02% (w/w) sodium azide (PBS/NaN_3) or protein solutions in PBS/NaN_3. Loading of Dextran Blue in the gels was established by co-dissolution of this

compound in the 2% (w/w) PEG_8–cholesterol/PEG_8–βCD solutions, followed by the aforementioned lyophilization and hydration procedure.

Rheological Experiments: Rheological characterization of the hydrogels was done with an AR-G2 rheometer (TA instruments, Etten-Leur, The Netherlands) equipped with a 1° steel cone geometry of 20-mm diameter and solvent trap. Using a spatula, approximately 55 μL sample was placed between the pre-heated (40 °C) plates of the rheometer. Rheological gel characteristics were monitored by oscillatory time sweep and temperature sweep experiments. During time sweep experiments the G' (shear storage modulus) and G'' (loss modulus) were measured at 37 °C for a period of 5 minutes. Temperature sweep experiments from 4 to 50 °C were done at a heating rate of 1 °C min^{-1} (30 s equilibration per point). The point at which $G''/G' (= \tan \delta) = 1$, is considered as the gel transition temperature (T_{gel}) [71]. All experiments were performed at a frequency of 1 Hz and 1% strain.

Swelling/Weight-Loss Experiments: Cylindrical hydrogels (300 mg, 6.5 × 9.0 mm (diameter × height)) with different percentages of solid content (15–35% (w/w)) were prepared in pre-weighed glass HPLC vials by hydration of the lyophilized polymer mixtures (45–105 mg) with appropriate volumes (195 to 255 μL) of PBS/NaN_3 for 16 hours at 4 °C. Next, 600 μL PBS/NaN_3 (pH 7.4) was added on top of the gels and the vials were incubated on a shaking plate at 37 °C. After regular time intervals, the buffer was removed to determine the weight of the gels, followed by the addition of fresh PBS/NaN_3. To measure the dry weight of the hydrogels in time, hydrogels were collected after regular time periods, lyophilized for 48 hours, and the weight of the residues were gravimetrically determined. To avoid the presence of salts after lyophilization, degradation was done in 5 mM NH_4OAc buffer (pH 4.7) instead of PBS/NaN_3.

Dextran Blue Release Experiments: 22.5% and 35% (w/w) cylindrical hydrogels (300 mg, 6.5 × 9.0 mm (diameter × height)) containing 1% (w/w) Dextran Blue were prepared in pre-weighed glass HPLC vials by hydration of the lyophilized mixtures (70.5 mg for 22.5% (w/w) gels; 108 mg for 35% (w/w) gels) composed of PEG_8–βCD, PEG_8–chol and Dextran Blue with appropriate volumes (229.5 μL for 22.5% (w/w) gels; 192 μL for 35% (w/w) gels) of PBS/NaN_3. Next, 600 μL PBS/NaN_3 (pH 7.4) was added on top of the gels and the vials were incubated on a shaking plate at 37 °C. At regular time intervals, the buffer was removed to determine the weight of the gels, followed by the addition of fresh PBS/NaN_3. The removed buffer samples were analyzed for its Dextran Blue content by measuring the absorbance at 620 nm with a Shimadzu UV-2450 spectrophotometer (Shimadzu Corporation, Kyoto, Japan) equipped with a 6-position cell holder.

Protein and Peptide Release Experiments: 22.5% and 35% (w/w) hydrogels (500 mg) containing 10 mg lysozyme, BSA, IgG, or 0.78 mg Bradykinin acetate per gram gel were prepared in 2 mL Eppendorf tubes as described in the hydrogel preparation section. After hydration, the gels were transferred into a previously described release device [62]. This device is made of polyoxymethylene and consists of a gel compartment (8.5 × 8.8 mm (diameter × height)) and a release compartment (15 × 30 mm (diameter × height)). To the gels (0.5 mL; 8.5 × 8.8 mm (diameter × height)), 3 mL PBS/NaN_3 was added as a release buffer, followed by incubation of the device on a shaking plate at 37 °C. At regular time points, aliquots of 0.5 mL release buffer were taken, followed by replacement of the aliquot with fresh buffer. Protein release samples were analyzed for their protein concentration using the BCA Protein Assay. To obtain calibration curves, standard protein solutions (concentration range 0.01–1 mg mL^{-1}) were prepared. Release samples (25 μL) were pipetted into a 96-microwells plate and 200 μL of working reagent (BCA reagent A:BCA reagent B, 50:1 v/v). After incubation of the plates for 30 minutes at 37 °C, the absorbance was measured at 550 nm with a Novapath Microplate Reader (Bio-Rad Laboratories, Hercules, USA). Bradykinin release samples were analyzed using a Waters Acquity Ultra Performance LC system (UPLC, Waters, Milford MA, USA) equipped with an Acquity BEH300 C18 1.7 μm column, a binary solvent manager, a sample manager with column oven at 50 °C, and an Acquity TUV Detector (detection wavelength: 210 nm). After injection of 10 μL release sample, a gradient was run from 100% A (H_2O/ACN 95/5 (% v/v) containing 0.1% TFA) to 30% B (100% ACN with 0.1% TFA) in 7 minutes at a flow rate of 1.0 mL min^{-1}. Peaks were detected at 210 nm. A calibration curve was obtained after injection of standard Bradykinin solutions (0.02–0.25 mg mL^{-1}). The chromatograms were analyzed using Empower Software Version 1154 (Waters, Milford MA, USA).

Determination of the Specific Enzymatic Activity of Lysozyme Released from the Gels: The enzymatic activity of lysozyme in the release samples was determined with an assay based on the hydrolysis of the outer cell membrane of *M. lysodeikticus*, which leads to solubilization of the affected bacteria and a detectable decrease of light scattering [72]. Lysozyme samples released from the different hydrogel compositions after 2, 5, and 7 days were used. These were then diluted to a lysozyme concentration of 30–60 μg mL^{-1}. Next, 10 μL of sample was added to 1.3 mL of *M. lysodeikticus* suspension (0.2 mg mL^{-1}, 66 mM phosphate buffer, pH 6.2) and the decrease in turbidity was measured for 200 s at 450 nm.

Fluorescence Recovery after Photobleaching (FRAP): The mobility of FITC-labeled BSA or FITC–lysozyme in 22.5% and 35% (w/w) PEG_8–βCD/PEG_8–chol gels was determined with fluorescence recovery measurements after photobleaching (FRAP). While FITC–BSA was used as provided by the supplier, lysozyme was labeled as previously reported [62]: 300 mg lysozyme and 12 mg FITC were each dissolved in 60 mL of a 0.1 M borate buffer (pH 8.6). While stirring, the FITC solution was added dropwise to the lysozyme solution and the resulting solution was stirred for 16 h. Next, the protein solution was extensively dialyzed for 7 days against water at 4 °C. FITC–lysozyme was collected by lyophilization. The extent of FITC-conjugation was 1.01 ± 0.08 mole FITC per mole lysozyme as determined by UV absorbance measurements at 494 and 280 nm [73].

Gels (150 mg) were made by hydration of the lyophilized polymer mixtures (see hydrogel preparation section) with a solution of FITC–lysozyme (1 mg · mL^{-1}) or FITC–BSA (2 mg · mL^{-1}) in 100 mM HEPES buffer (pH 7.0). As a control, the FITC-labeled proteins were dissolved in solutions of non-functionalized 8-arm PEG (22.5% and 35% (w/w) PEG_8–OH). Next, a spatula tip of the fluorescent protein-loaded hydrogels was placed on a microscope glass slide, on which an adhesive spacer (Secure-Seal Spacer, Molecular Probes, Leiden, The Netherlands) of 0.5-mm thickness (adhering at both sides) was fixed, followed by the attachment of a cover glass. FRAP measurements (at 37 °C) were performed using a setup as described previously [63,74]. In detail, a confocal scanning laser microscope (model MRC1024 UV, Bio-Rad, Hemel Hempstead, UK) modified for bleaching arbitrary regions, was used with a 10× NA 0.45 objective lens (CFI Plan Apochromat; Nikon, Badhoevedorp, The Netherlands). The 488-nm line of a 4 W Argon ion laser (model Stabilite 2017; Spectra-Physics, Darmstadt, Germany) was used to bleach uniform disks with a diameter between 20 and 80 μm. The bleaching phase was very short (200 ms) so that the extent of fluorescence recovery that will take place during the bleaching phase is negligible. After photobleaching, 30 to 50 images were acquired at regular time intervals with a highly attenuated laser beam for measuring the fluorescence recovery in the bleached area, which is due to the diffusion of fluorescently labeled protein molecules from the surrounding unbleached area into the bleached region. The diffusion coefficient can be calculated from the experimental recovery curve by fitting of the appropriate FRAP model [63].

Acknowledgements

This research was financially supported by a grant of the Ministry of Economic Affairs, The Netherlands (SenterNovem IS042016). Supporting Information is available online from Wiley InterScience or from the author.

Received: April 8, 2009
Published online: July 24, 2009

[1] N. A. Peppas, P. Bures, W. Leobandung, H. Ichikawa, *Eur. J. Pharm. Biopharm.* **2000**, *50*, 27.
[2] N. A. Peppas, J. Z. Hilt, A. Khademhosseini, R. Langer, *Adv. Mater.* **2006**, *18*, 1345.
[3] F. Brandl, F. Sommer, A. Goepferich, *Biomaterials* **2007**, *28*, 134.

[4] N. E. Fedorovich, J. Alblas, J. R. de Wijn, W. E. Hennink, A. J. Verbout, W. J. A. Dhert, *Tissue Eng.* **2007**, *13*, 1905.
[5] W. E. Hennink, C. F. van Nostrum, *Adv. Drug Delivery Rev.* **2002**, *54*, 13.
[6] T. R. Hoare, D. S. Kohane, *Polymer* **2008**, *49*, 1993.
[7] A. S. Hoffman, *Adv. Drug Delivery Rev.* **2002**, *54*, 3.
[8] C. C. Lin, A. T. Metters, *Adv. Drug Delivery Rev.* **2006**, *58*, 1379.
[9] S. J. Bryant, C. R. Nuttelman, K. S. Anseth, *J. Biomater. Sci, Polym. Ed.* **2000**, *11*, 439.
[10] C. C. Lin, A. T. Metters, *Biomacromolecules* **2008**, *9*, 789.
[11] C. G. Williams, A. N. Malik, T. K. Kim, P. N. Manson, J. H. Elisseeff, *Biomaterials* **2005**, *26*, 1211.
[12] S. R. Van Tomme, G. Storm, W. E. Hennink, *Int. J. Pharm.* **2008**, *355*, 1.
[13] C. B. Packhaeuser, J. Schnieders, C. G. Oster, T. Kissel, *Eur. J. Pharm. Biopharm.* **2004**, *58*, 445.
[14] J. D. Kretlow, L. Klouda, A. G. Mikos, *Adv. Drug Delivery Rev.* **2007**, *59*, 263.
[15] A. Hatefi, B. Amsden, *J. Controlled Release* **2002**, *80*, 9.
[16] K. Y. Lee, J. A. Rowley, P. Eiselt, E. M. Moy, K. H. Bouhadir, D. J. Mooney, *Macromolecules* **2000**, *33*, 4291.
[17] S. R. Van Tomme, M. J. van Steenbergen, S. C. De Smedt, C. F. van Nostrum, W. E. Hennink, *Biomaterials* **2005**, *26*, 2129.
[18] S. Hietala, P. Mononen, S. Strandman, P. Jarvi, M. Torkkeli, K. Jankova, S. Hvilsted, H. Tenhu, *Polymer* **2007**, *48*, 4087.
[19] B. Jeong, Y. H. Bae, D. S. Lee, S. W. Kim, *Nature* **1997**, *388*, 860.
[20] T. Vermonden, N. A. M. Besseling, M. J. van Steenbergen, W. E. Hennink, *Langmuir* **2006**, *22*, 10180.
[21] B. O. Haglund, R. Josi, K. J. Himmelstein, *J. Controlled Release* **1996**, *41*, 229.
[22] Y. J. Wang, L. M. Tang, H. Yu, *J. Colloid Interface Sci.* **2008**, *319*, 357.
[23] R. J. H. Stenekes, H. Talsma, W. E. Hennink, *Biomaterials* **2001**, *22*, 1891.
[24] H. J. Chung, Y. H. Lee, T. G. Park, *J. Controlled Release* **2008**, *127*, 22.
[25] S. J. de Jong, S. C. De Smedt, M. W. C. Wahls, J. Demeester, J. J. Kettenes-van den Bosch, W. E. Hennink, *Macromolecules* **2000**, *33*, 3680.
[26] S. J. de Jong, W. N. E. van Dijk-Wolthuis, J. J. Kettenes-van den Bosch, P. J. W. Schuyl, W. E. Hennink, *Macromolecules* **1998**, *31*, 6397.
[27] C. Hiemstra, Z. Y. Zhong, P. Dijkstra, J. Feijen, *Macromol. Symp.* **2005**, *224*, 119.
[28] K. L. Kiick, *Soft Matter* **2008**, *4*, 29.
[29] T. Miyata, N. Asami, T. Uragami, *Nature* **1999**, *399*, 766.
[30] S. Nagahara, T. Matsuda, *Polymer Gels and Networks* **1996**, *4*, 111.
[31] F. van de Manakker, M. van der Pot, T. Vermonden, C. F. van Nostrum, W. E. Hennink, *Macromolecules* **2008**, *41*, 1766.
[32] F. van de Manakker, T. Vermonden, N. el Morabit, C. F. van Nostrum, W. E. Hennink, *Langmuir* **2008**, *24*, 12559.
[33] A. Charlot, R. Auzely-Velty, *Macromolecules* **2007**, *40*, 1147.
[34] A. Hashidzume, I. Tomatsu, A. Harada, *Polymer* **2006**, *47*, 6011.
[35] O. Kretschmann, S. W. Choi, M. Miyauchi, I. Tomatsu, A. Harada, H. Ritter, *Angew. Chem, Int. Ed.* **2006**, *45*, 4361.
[36] L. Soltes, R. Mendichi, G. Kogan, M. Mach, *Chem. Biodiversity* **2004**, *1*, 468.
[37] M. Weickenmeier, G. Wenz, J. Huff, *Macromol. Rapid Commun.* **1997**, *18*, 1117.
[38] T. Loftsson, D. Duchene, *Int. J. Pharm.* **2007**, *329*, 1.
[39] D. Harries, D. C. Rau, V. A. Parsegian, *J. Am. Chem. Soc.* **2005**, *127*, 2184.
[40] L. Liu, Q. X. Guo, *J. Inclusion Phenom. Macrocyclic Chem.* **2002**, *42*, 1.
[41] M. V. Rekharsky, Y. Inoue, *Chem. Rev.* **1998**, *98*, 1875.
[42] A. Charlot, R. Auzely-Velty, M. Rinaudo, *J. Phys. Chem. B* **2003**, *107*, 8248.
[43] A. Charlot, R. Auzely-Velty, *Macromolecules* **2007**, *40*, 9555.
[44] W. N. E. van Dijk-Wolthuis, J. A. M. Hoogeboom, M. J. van Steenbergen, S. K. Y. Tsang, W. E. Hennink, *Macromolecules* **1997**, *30*, 4639.
[45] J. L. West, J. A. Hubbell, *React. Polym.* **1995**, *25*, 139.
[46] S. J. de Jong, B. van Eerdenbrugh, C. F. van Nostrum, J. J. Kettenes-van den Bosch, W. E. Hennink, *J. Controlled Release* **2001**, *71*, 261.
[47] P. van de Wetering, A. T. Metters, R. G. Schoenmakers, J. A. Hubbell, *J. Controlled Release* **2005**, *102*, 619.
[48] S. G. Levesque, M. S. Shoichet, *Bioconjugate Chem.* **2007**, *18*, 874.
[49] M. A. Rice, J. Sanchez-Adams, K. S. Anseth, *Biomacromolecules* **2006**, *7*, 1968.
[50] M. P. Lutolf, J. L. Lauer-Fields, H. G. Schmoekel, A. T. Metters, F. E. Weber, G. B. Fields, J. A. Hubbell, *Proc. Natl. Acad. Sci. USA.* **2003**, *100*, 5413.
[51] M. P. Lutolf, G. P. Raeber, A. H. Zisch, N. Tirelli, J. A. Hubbell, *Adv. Mater.* **2003**, *15*, 888.
[52] J. Tamada, R. Langer, *J. Biomater. Sci, Polym. Ed.* **1992**, *3*, 315.
[53] A. C. Albertsson, M. Eklund, *J. Appl. Polym. Sci.* **1995**, *57*, 87.
[54] J. Heller, *Biomaterials* **1990**, *11*, 659.
[55] G. Tae, J. A. Kornfield, J. A. Hubbell, D. Johannsmann, T. E. Hogen-Esch, *Macromolecules* **2001**, *34*, 6409.
[56] Y. Cao, H. B. Li, *Chem. Commun.* **2008**, 4144.
[57] W. Shen, K. C. Zhang, J. A. Kornfield, D. A. Tirrell, *Nat. Mater.* **2006**, *5*, 153.
[58] B. Jeong, Y. H. Bae, S. W. Kim, *Macromolecules* **1999**, *32*, 7064.
[59] R. Jin, C. Hiemstra, Z. Zhong, J. Feijen, *Biomaterials* **2007**, *28*, 2791.
[60] P. L. Ritger, N. A. Peppas, *J. Controlled Release* **1987**, *5*, 23.
[61] L. Serra, J. Domenech, N. A. Peppas, *Biomaterials* **2006**, *27*, 5440.
[62] S. R. Van Tomme, B. G. De Geest, K. Braeckmans, S. C. De Smedt, F. Siepmann, J. Siepmann, C. F. van Nostrum, W. E. Hennink, *J. Controlled Release* **2005**, *110*, 67.
[63] K. Braeckmans, L. Peeters, N. N. Sanders, S. C. De Smedt, J. Demeester, *Biophys. J.* **2003**, *85*, 2240.
[64] K. Burczak, T. Fujisato, M. Hatada, Y. Ikada, *Biomaterials* **1994**, *15*, 231.
[65] E. W. Merrill, K. A. Dennison, C. Sung, *Biomaterials* **1993**, *14*, 1117.
[66] P. W. Atkins, J. de Paula, *Atkins' Physical Chemistry*, Oxford University Press, New York, USA **2002**, Ch. 24.
[67] N. A. Peppas, C. T. Reinhart, *J. Membr. Sci.* **1983**, *15*, 275.
[68] Y. Inoue, T. Hakushi, Y. Liu, L. H. Tong, B. J. Shen, D. S. Jin, *J. Am. Chem. Soc.* **1993**, *115*, 475.
[69] F. Jara, M. Dominguez, M. C. Rezende, *Tetrahedron* **2006**, *62*, 7817.
[70] S. Wang, Y. Dai, T. Fukuoka, H. Yamanaka, K. Kobayashi, K. Obata, X. Y. Cui, M. Tominaga, K. Noguchi, *Brain* **2008**, *131*, 1241.
[71] H. H. Winter, *Polym. Eng. Sci.* **1987**, *27*, 1698.
[72] P. Shih, B. A. Malcolm, S. Rosenberg, J. F. Kirsch, A. C. Wilsow, *Methods Enzym.* **1993**, *224*, 576.
[73] T. Konecsni, F. Kilár, *J. Chromatogr, A* **2004**, *1051*, 135.
[74] S. C. De Smedt, T. K. L. Meyvis, J. Demeester, P. Van Oostveldt, J. C. G. Blonk, W. E. Hennink, *Macromolecules* **1997**, *30*, 4863.